Occurrence of incoherent α"-$Fe_{16}N_2$ at room temperature in iron-nitrogen martensite observed by neutron and X-ray diffraction

1990 J. Phys.: Condens. Matter 2 9237

(http://iopscience.iop.org/0953-8984/2/47/001)

J. Phys.: Condens. Matter **2** (1990) 9237–9245. Printed in the UK

Occurrence of incoherent α''-$Fe_{16}N_2$ at room temperature in iron–nitrogen martensite observed by neutron and x-ray diffraction

A Böttger†, Liu Cheng†, E Frikkee‡, Th H de Keijser† and E J Mittemeijer†

† Delft University of Technology, Laboratory of Metallurgy, Rotterdamseweg 137, 2628 AL Delft, The Netherlands

‡ Netherlands Energy Research Foundation ECN, PO Box 1,1755 ZG, Petten, The Netherlands

Received 11 December 1989, in final form 25 July 1990

Abstract. Aging behaviour of iron–nitrogen martensite (about 5 at.% N) at room temperature is investigated by neutron and x-ray diffraction experiments. An attempt is made to reveal the configuration of the nitrogen atoms during the aging processes especially by means of neutron diffraction, since the scattering lengths of iron and nitrogen atoms are almost the same.

Two successive processes are distinguished: a *redistribution* of nitrogen atoms in the iron matrix and the *formation* of incoherent $Fe_{16}N_2$. During about the first 40 h of aging a decrease in the integrated intensity (10–20%) of the neutron and x-ray {002} martensite reflection is observed. This reduction is ascribed to the change in mean square displacement of *iron* atoms close to occupied interstices within nitrogen-enriched regions. After only about 1 d of aging, incoherent $Fe_{16}N_2$ has already formed. The changes in the integrated intensities of the precipitate and martensite reflections indicate that, during the precipitation process, $Fe_{16}N_2$ and ferrite are formed locally while the nitrogen content of the remaining martensite is unchanged.

1. Introduction

Iron–nitrogen and iron–carbon martensites (α') appear to be similar in many respects. For instance, their structure can be described as a body-centred tetragonal (BCT) iron lattice with (dominantly) the '*c*-type' octahedral interstices occupied by nitrogen or carbon atoms. Also the effective sizes of the interstitial atoms are about the same. A recent evaluation of data in the literature indicated that the *c* lattice parameters are identical for both systems and that there is possibly a minute difference in the *a* lattice parameters [1]. Comparable stages of tempering have been identified: first a transition nitride (α'')–carbide (ε, η) develops, which on continued tempering is converted into an 'equilibrium' nitride (γ')–carbide (cementite, θ). Recent research has been focused on the processes preceding the first stage: the pre-precipitation processes which involve the redistribution of interstitials. In particular, in this stage of aging, the behaviours of both martensites appear to be quite different [2].

0953-8984/90/479237 + 09 $03.50

The transition nitride α''-$Fe_{16}N_2$ is almost isostructural with the parent martensite; the α''-unit cell comprises $2 \times 2 \times 2$ tetragonal unit cells of martensite in which the nitrogen atoms are distributed in an ordered way [3]. The development of α''-regions involves only the redistribution of nitrogen atoms. The structure of the transition carbide is, however, more complicated [4, 5] and thus its precipitation requires the redistribution of both carbon and iron atoms.

Here, the results of a study of (pre-)precipitation processes in iron–nitrogen martensite upon aging at room temperature are presented. Two different methods of investigation are used: neutron and x-ray diffraction. Both methods allow the observation of structural changes in a material although the origin of the scattering is different. In the x-ray diffraction measurements, phase transformations are probed through changes in the iron lattice, because iron atoms dominate the scattering process. The nuclear scattering lengths of iron and nitrogen for neutrons are, on the other hand, comparable. Therefore structural changes in the nitrogen configuration can, in principle, be observed more readily by neutron diffraction.

2. Experimental conditions

2.1. Sample preparation

Thin iron–nitrogen martensitic sheets (10^{-2} m $\times$ 10^{-2} m $\times$ 10^{-4} m) were made by nitriding pure iron at 1023 K in a gas flow of 96 vol.% NH_3–4 vol.% H_2 as described in more detail in [6]. The nitrogen content of the martensite, determined by the change in weight on nitriding, is about 5 at.%. The thickness of the sheets is limited by the condition that a homogeneous distribution of dissolved nitrogen in the Fe matrix is required. Thicker foils need a longer nitriding time, which leads to the formation of pores filled with N_2 gas near the surface of the foils [7]. Martensite was formed by quenching the samples in brine and, subsequently, in liquid nitrogen.

2.2. Neutron diffraction

In order to obtain a sufficiently large sample for the neutron scattering experiment, seven martensitic sheets were clenched together in an aluminium sample holder, covered with a cadmium sheet 10^{-3} m thick on one side. The latter prevents scattering from the sample holder. To prevent the martensite from aging during the measurements (total 600 h), the specimen was kept at $T = 170$ K in a variable-temperature liquid-N_2 cryostat. During the aging periods the sample was kept at room temperature (293 K). The total aging time of 537 h was interrupted 11 times for the recording of a diffraction scan.

The neutron diffraction experiments were performed with a triple-axis spectrometer (high-flux reactor, Petten). A wavelength λ of 0.14259 nm was selected from the incident (unpolarized) beam by a pyrolytic graphite monochromator. A pyrolytic graphite analyser was installed to suppress the diffraction peaks resulting from the higher-order (λ/n) contamination in the beam. Soller slit collimators of 30′ and 15′ were placed in front of the monochromator and the analyser, respectively.

After each aging period, several $\{hkl\}$ peaks were examined: the $\{011\}_{\alpha'}$–$\{110\}_{\alpha'}$ and $\{002\}_{\alpha'}$–$\{200\}_{\alpha'}$ martensite doublet reflections, the $\{002\}_{\gamma}$ austenite (γ) reflection and the $\{004\}_{\alpha''}$–$\{400\}_{\alpha''}$ nitride doublet reflections. During the second stage of aging (formation of incoherent α''; see section 3.3), the diffraction pattern becomes rather complicated because it consists of several overlapping reflections. From the crystallographic data in

Table 1. Crystallographic data, X_N is the atomic percentage of nitrogen.

Phase	Structure	Lattice parameter (nm)	Reference
Martensite (α')	BCT	$a = 0.28664 - 0.00018X_N$ $c = 0.28664 + 0.00263X_N$	[1]
Ferrite (α)	BCC	0.28664	[8]
α''-$Fe_{16}N_2$	BCT	$a = 0.572$ $c = 0.629$	[3]

table 1 it can be deduced that the peak designated as the '$\{200\}_{\alpha'}$' reflection is composed of the following unresolved components: $\{200\}_{\alpha'}$–$\{020\}_{\alpha'}$, $\{400\}_{\alpha''}$–$\{040\}_{\alpha''}$ and $\{200\}_{\alpha}$.

The diffraction pattern was recorded in the 2θ range from 40° to 65° in steps of 0.22°. Fluctuations (about 4%) in the incident neutron flux were taken into account by controlling the observation time such that a preselected fixed number of neutrons (1.5×10^5 per step) were counted in the monitor detector in the incoming beam. In the 2θ range from 15° to 40° the observation time was increased (monitor preset at 8×10^5) in an attempt to observe the very weak $\{002\}_{\alpha''}$ reflection of $Fe_{16}N_2$. The data were normalized to a preset of 10^5 incoming neutrons, and the intensity contribution of the sample frame and cryostat was subtracted. The line profiles were fitted by a gaussian function and a background estimated by linear interpolation between the extremities of the diffraction peak (Siemens Diffrac 11 software).

2.3. X-ray diffraction

Since the x-ray diffraction experiments are described in detail in [9], only a short survey of their main features are given. The x-ray (Cr Kα) diffraction experiments were performed on a Siemens D-500 diffractometer with a graphite monochromator in the diffracted beam. During the measurements the specimen stayed at room temperature. About 18 measurements were made after aging for between 0.8 and 672 h at room temperature (297 K). The diffraction pattern in the 2θ range from 85° to 164° was measured in steps of 0.2° (2θ) which resulted in a total measuring (aging) time of 2 h for each experiment. This angular range includes the $\{011\}_{\alpha'}$–$\{110\}_{\alpha'}$, the $\{002\}_{\alpha'}$–$\{200\}_{\alpha'}$, the $\{004\}_{\alpha''}$–$\{400\}_{\alpha''}$ and $\{112\}_{\alpha'}$–$\{211\}_{\alpha'}$ doublets, and the $\{220\}_{\gamma}$ reflection. The diffraction profiles were fitted by pseudo-Voigt functions as implemented in the Siemens software package Diffrac 11.

3. Results and interpretation

From both the neutron and the x-ray diffraction profiles the integrated intensities and the peak positions after different aging times were determined. The peak positions obtained from the neutron diffraction experiments turned out to be less accurate than those obtained from x-ray diffraction experiments, because of the presence of weak aluminium {200} and {220} reflections from unshielded cryostat parts, close to the α' diffraction peaks. The following discussion of structural changes is based in particular on the $\{002\}_{\alpha'}$–$\{200\}_{\alpha'}$ doublet reflection, since this doublet is well resolved and measured in both experiments. The data obtained from the (less resolved) other doublets are

consistent with those from the $\{002\}_{\alpha'}$–$\{200\}_{\alpha'}$ doublet. The $\{200\}_{\gamma}$ reflection did not change within experimental accuracy.

First the main difference between x-ray and neutron scattering is mentioned briefly. For x-rays the scattering is caused by the interaction with the electrons in the material. For the $\{002\}_{\alpha'}$–$\{200\}_{\alpha'}$ doublet, the scattering power of iron is about six times the scattering power of nitrogen [10] ($2\theta = 100°$; Cr Kα). On the other hand, the scattering of neutrons is due to the interaction with the nuclei and the unpaired electron spins (magnetic moments) of the atoms [11]. The nuclear scattering lengths of iron and of nitrogen are about the same. In the estimation of the magnetic contribution of the iron atoms to the integrated intensity of the $\{002\}_{\alpha'}$–$\{200\}_{\alpha'}$ doublet it is assumed that the magnetic moments and the magnetic form factors of martensite are the same as in α-Fe [12]. The intensity of the magnetic scattering depends on the orientation of the magnetic moments with respect to the scattering vector [11]. Since the c axis is the preferred direction of the magnetization†, the contribution to the $\{200\}_{\alpha'}$ reflection is 4% (maximum value) of the nuclear part, and the $\{002\}_{\alpha'}$ reflection does not contain a magnetic part.

In comparing the results of the neutron and x-ray diffraction, three additional differences in the experimental conditions are of importance, namely the differences in sample temperature (170 K versus 297 K), the penetration depth, and the scattering geometry (transmission versus reflection geometry). An additional neutron diffraction scan at 140 K (aging time 300 h) revealed that the integrated intensity of the $\{002\}_{\alpha'}$ peak and that of the $\{200\}_{\alpha'}$ peak increase with different amounts (13% and 6%, respectively, with respect to the experiment at 170 K) upon decreasing temperature. This indicates that the temperature factor is considerable and anisotropic.

In the transmission geometry used for the neutron diffraction experiments, the $\{002\}_{\alpha'}$ and $\{200\}_{\alpha'}$ lattice planes of the diffracting crystallites have an inclination of about 60° with respect to the specimen surface. Whereas for the reflection geometry used for the x-ray experiments, only the crystallites with lattice planes parallel to the surface contribute to the diffraction. The present x-ray diffraction set-up only probes surface-adjacent material; the information depth [14] is about 4 μm. For neutron diffraction, on the other hand, all depths of the specimen (thickness about 700 μm) contribute almost 'equally' to the diffraction.

3.1. The as-quenched state

In the as-quenched state the ratio ($I_{\alpha'}^{200}/I_{\alpha'}^{002}$) of the integrated intensities of the $\{200\}_{\alpha'}$ to the $\{002\}_{\alpha'}$ neutron diffraction reflections obtained by linear extrapolation (least-squares fit) to zero aging time equals 2.1 ± 0.1 (figure 1). In a first approximation based on the mutiplicity and Lorentz factors an intensity ratio of 1.86 is expected for a random occupation of the a, b and c octahedral sites. However, the static displacement of the iron atoms caused by the dominant occupation of 'c-type' octahedral interstices attenuate in particular the $\{002\}_{\alpha'}$ reflection, as is discussed for Fe–C martensite in [15, 16]. Hence, as a consequence of the anisotropy of the temperature effect, the magnetic scattering (see above) and the static displacements, an intensity ratio larger than 1.86 is expected. The x-ray diffraction data yield an intensity ratio of about 1. In

† From a Rietveld refinement of the data [13] obtained after an aging time of 20 h and of 537 h it was obvious that there is no magnetic moment in the (a, b) plane.

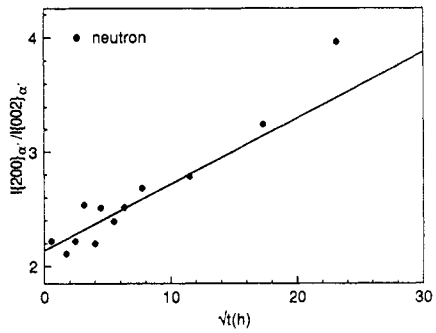

Figure 1. The ratio of the integrated intensities of the $\{200\}_{\alpha'}$ to $\{002\}_{\alpha'}$ reflections versus the square root of the aging time at room temperature. The straight line is a least-squares fit through data obtained for aging times $t < 40$ h.

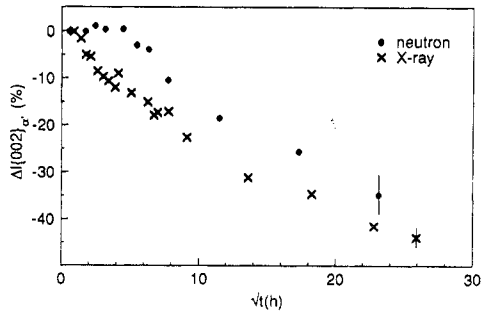

Figure 2. The relative change (compared with the first measurement) of the integrated intensity of the $\{002\}_{\alpha'}$ reflection versus the square root of the aging time at room temperature. Error bars ($\pm\sigma$) are indicated for each set of data points.

view of the limited information depth for x-ray diffraction experiments, this could be caused by the presence of texture in the surface regions of the specimen.

3.2. The pre-precipitation processes

Three processes involving diffusion of nitrogen atoms are distinguished, namely segregation, transfer from *a* and *b* octahedral interstices to *c* octahedral interstices and ordering–clustering [9]. In the segregation and transfer processes a very small amount of nitrogen atoms (about 0.1 at.% N) is involved, as is discussed in [9]. The major part of the interstitials forms local enrichments of nitrogen in the iron matrix. This increases the mean square static atomic displacement in the iron matrix, while the mean static atomic displacement can remain unchanged [16]. This holds in the case of 'ordering' (ordered occupation of octahedral interstices) as well as in the case of clustering (random occupation of octahedral interstices) of nitrogen atoms. The effect of the mean square static displacement on the intensity is comparable with that of the mean square dynamic displacement due to thermal vibration [17]. Thus, the development of local enrichments of nitrogen reduces the intensity of reflections. Since the nitrogen atoms mainly occupy '*c*-type' octahedral interstices, in particular the integrated intensity of the $\{002\}_{\alpha'}$ reflection is expected to be attenuated during the pre-precipitation process. Figure 2 shows that, in about the first 40 h of aging, the $\{002\}_{\alpha'}$ integrated intensity decreases significantly (for the decrease on continued aging, see section 3.3). Further, the neutron $\{002\}_{\alpha'}$ integrated intensity is initially constant whereas the x-ray $\{002\}_{\alpha'}$ integrated intensity is attenuated from the start onwards. The reason for this difference in behaviour is not understood at the moment but a difference in treatment of the specimens (repeated cooling and heating of the sample used for neutron diffraction) or a change in the contribution of the magnetic scattering may influence the intensities.

3.3. The formation of incoherent α″

Neutron and x-ray diffraction data indicate that, after aging for about one day at room temperature, incoherent precipitates of α''-$Fe_{16}N_2$ develop. On the small-angle side of

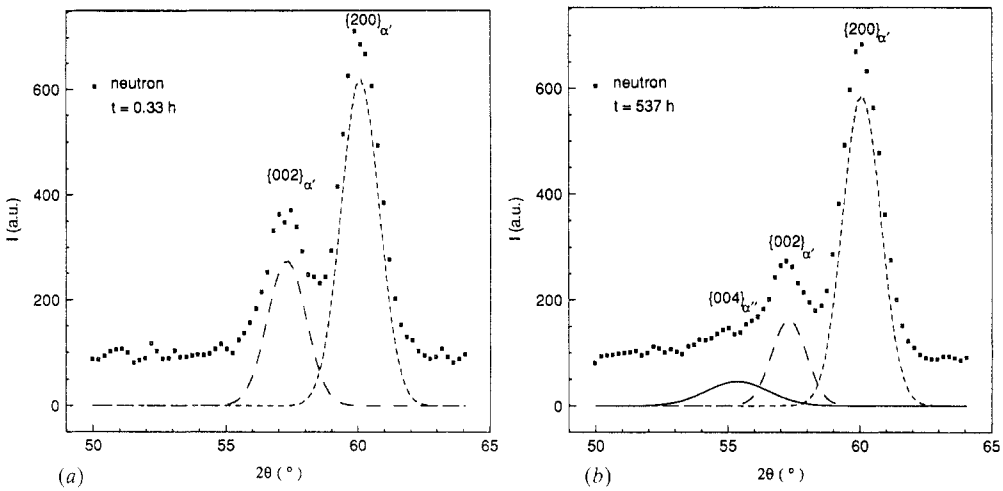

Figure 3. Neutron diffractograms of the $\{002\}_{\alpha'}$–$\{200\}_{\alpha'}$ doublet after aging for (*a*) 0.33 h and (*b*) for 537 h at room temperature. The profiles indicated are obtained from a pattern decomposition by using gaussian fit functions.

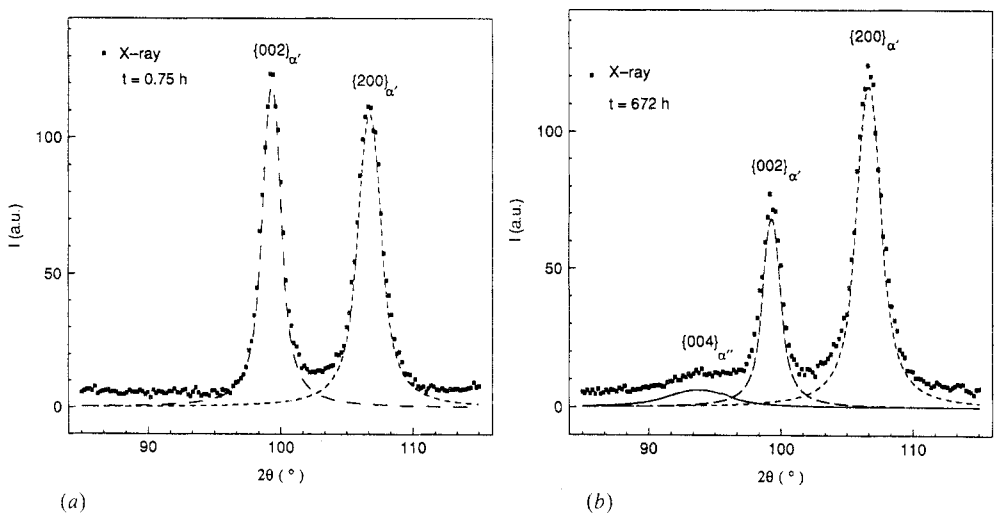

Figure 4. X-ray diffractograms of the $\{002\}_{\alpha'}$–$\{200\}_{\alpha'}$ doublet after aging for (*a*) 0.75 h and (*b*) for 672 h at room temperature. The profiles indicated are obtained from a pattern decomposition by using pseudo-Voigt fit functions.

the $\{002\}_{\alpha'}$–$\{200\}_{\alpha'}$ doublet a diffraction peak emerges which can be indexed as $\{004\}_{\alpha''}$ (figures 3 and 4). The occurrence of the $\{004\}_{\alpha''}$ peak implies that the iron and nitrogen atoms in regions containing an ordered arrangement of nitrogen atoms now diffract independently from the matrix. Because of the orientation relationship between α' and α'', implying that $(001)_{\alpha'} \| (001)_{\alpha''}$ [18] and the diffraction geometries used, the atoms contributing to the $\{004\}_{\alpha''}$ reflection in this stage of aging contributed in the redistribution stage to the $\{002\}_{\alpha'}$ reflection. The increase in the integrated intensity of the $\{004\}_{\alpha''}$

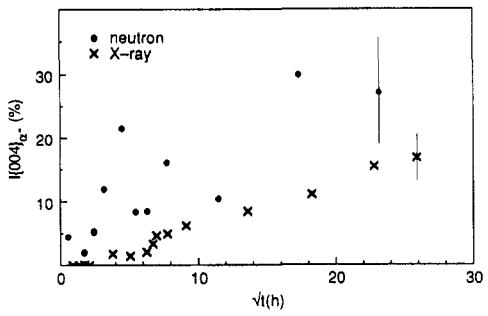

Figure 5. The ratio of the integrated intensity of the $\{004\}_{\alpha''}$ precipitate reflection and the first measurement of the $\{002\}_{\alpha'}$ integrated intensity versus the square root of the aging time at room temperature. Error bars ($\pm\sigma$) are indicated for each set of data points.

reflection is shown in figure 5; the decrease in the integrated intensity of the $\{002\}_{\alpha'}$ reflection is shown in figure 2.

In what follows, the relation between the increase of the integrated intensity of the $\{004\}_{\alpha''}$ and the decrease in the $\{002\}_{\alpha'}$ integrated intensity will be discussed. The integrated intensity of a reflection is, in general, given by [19]

$$I_i^{hkl} \propto (N_i/v_i)|F_i^{hkl}|^2 \text{ LP} \tag{1}$$

where N_i is the number of unit cells of phase i ($=\alpha', \alpha''$) contained in the effective diffracting volume (the absorption coefficient does not change by the phase transformation), v_i is the unit cell volume, F_i^{hkl} is the structure factor of the $\{hkl\}$ reflection and LP is the Lorentz (polarization) factor. Let $X_{\alpha'}$ and $X_{\alpha''}$ denote the number of nitrogen atoms per 100 iron atoms of α' and α'', respectively. If the precipitation reaction is such that α' converts into α'' and α (ferrite), then the precipitation of one unit cell of α'' requires that $8X_{\alpha''}/X_{\alpha'}$ unit cells of α' are converted. This can be seen from an atom balance; note that it is assumed that the ferrite contains no nitrogen atoms. Thus, for any stage of the transformation $\alpha' \rightarrow \alpha'' + \alpha$, the ratio of the changes in the integrated intensities becomes

$$|\Delta I_{\alpha'}^{002}/\Delta I_{\alpha''}^{004}| = (8X_{\alpha''}|F_{\alpha'}^{002}|^2 v_{\alpha''})/(X_{\alpha'}|F_{\alpha''}^{004}|^2 v_{\alpha'}) \tag{2}$$

where it is assumed that the Lorentz (polarization) factors are equal for both reflections and that the intensity reductions due to the static displacement of the iron atoms around the interstitials are equal for both reflections. The latter assumption is based on the following consideration: the mean square static displacement of the iron atoms in the c direction is expected to be larger for α'' than for α' because $X_{\alpha''} > X_{\alpha'}$; however, the formation of α'' is associated with a reduction in elastic strain energy [20] and thus with a reduction in the mean square static displacement (also a small dilatation occurs during precipitation of incoherent α'' [6]).

The intensity changes of the $\{002\}_{\alpha'}$ reflection in the first stage of aging (up to about 40 h) are dominated by the pre-precipitation processes (cf section 3.2). Therefore, to verify the precipitation model underlying equation (2), the intensity changes will be taken relative to the intensities recorded after aging for 60 h. The experimental values of the ratios $|\Delta I_{\alpha'}^{002}/\Delta I_{\alpha''}^{004}|$ thus obtained (average obtained from the two longest aging times) are 2.2 ± 0.5 for neutron scattering and 2.2 ± 0.2 for x-ray scattering. They are in agreement with the calculated values: 2.2 for the neutron specimen containing 5 at.% N and 2.1 for the x-ray specimen containing 5.8 at.% N near the surface [9], using data from the literature [10] for the scattering factors of nitrogen and iron. If the nitrogen content of the martensite matrix were to decrease *gradually*, an intensity ratio of about

one is expected. Also a shift and broadening of the $\{002\}_{\alpha'}$ reflection towards larger Bragg angles is then expected because the c lattice parameter of α' is in particular sensitive to the nitrogen content. This is not consistent with experiment.

The agreement observed earlier between the predicted and experimental intensity ratios justifies the precipitation model considered: $\alpha' \rightarrow \alpha'' + \alpha$. This suggests that the α'' particles are surrounded by ferrite. Clearly the local depletion of nitrogen from the martensite by α'' precipitation is not supplemented by long-range diffusion of nitrogen atoms. In this context it is noted that, at room temperature, the diffusion distance ($\sqrt{2Dt}$) of nitrogen in ferrite as calculated from data in [21] is about 50 nm for an aging time of one day.

Finally, we remark that the presence of α''-$Fe_{16}N_2$ implies that in principle the $\{002\}_{\alpha''}$–$\{200\}_{\alpha''}$ doublet might be observed too. Since the interstitial nitrogen atoms in the α'' phase form a BCT sublattice with c and a parameters about twice that of the BCT martensite matrix [3], this $\{002\}_{\alpha''}$–$\{200\}_{\alpha''}$ doublet occurs at about the angular position of the 'forbidden' $\{001\}_{\alpha'}$–$\{100\}_{\alpha'}$ martensite reflection. Hence, already in the redistribution stage, in the case when ordering of nitrogen occurs, this reflection can appear. Local enrichment involving a random occupation of the interstices will only reduce the $\{002\}_{\alpha'}$/$\{200\}_{\alpha'}$ intensity. Since only scattering of nitrogen contributes to the $\{002\}_{\alpha''}$ reflection, even in the case of nitrogen-'sensitive' neutron diffraction the integrated intensity of the $\{002\}_{\alpha''}$ diffraction peak is only about 1% of the $\{004\}_{\alpha''}$ integrated intensity. Thus the $\{002\}_{\alpha''}$–$\{200\}_{\alpha''}$ doublet is expected to be extremely weak. The present set-up did not allow unambiguous detection of the $\{002\}_{\alpha''}$, not even when incoherent α'' occurred, since the $\lambda/2$ contamination (about 10%) of the incident beam gave rise to $\{002\}_{\alpha'}$–$\{200\}_{\alpha'}$ reflections close to the $\{002\}_{\alpha''}$–$\{200\}_{\alpha''}$ reflections, and with an intensity of the same order as the calculated intensity of the $\{002\}_{\alpha''}$–$\{200\}_{\alpha''}$ reflection.

4. Conclusions

(i) During the first 40 h of aging at room temperature a pronounced decrease in the integrated intensity of the $\{002\}_{\alpha'}$ reflection occurs. This decrease is ascribed to the formation of local nitrogen enrichments containing nitrogen dominantly in 'c-type' octahedral interstices. The initial changes in the integrated intensity of the $\{002\}_{\alpha'}$ reflections observed by neutron and by x-ray diffraction appear to be different; the attenuation of the $\{002\}_{\alpha'}$ integrated intensity during the first 25 h of aging as observed by neutron diffraction is less than the change observed by x-ray diffraction.

(ii) The neutron diffraction experiments as well as the x-ray diffraction experiments show that incoherent α'' precipitates develop during prolonged aging at room temperature. In both experiments a diffraction peak arises close to the $\{002\}_{\alpha'}$–$\{200\}_{\alpha'}$ doublet, which can be indexed as the $\{004\}_{\alpha''}$ reflection. Moreover, the decrease in the integrated intensity of the $\{002\}_{\alpha'}$ reflection and the increase in the integrated intensity of the $\{004\}_{\alpha''}$ reflection are quantitatively consistent with the local decomposition of martensite into α'' and α.

References

[1] Liu Cheng, Böttger A, de Keijser Th H and Mittemeijer E J 1990 *Scr. Mater.* **24** 509
[2] Mittemeijer E J, Liu Cheng, van der Schaaf P J, Brakman C J and Korevaar B M 1988 *Metall. Trans.* A **19** 925
[3] Jack K H 1943 *Proc. R. Soc.* A **208** 216
[4] Jack K H 1951 *J. Iron Steel Inst.* **169** 26

[5] Hirotsu Y and Nagakura S 1972 *Acta Metall.* **20** 645
[6] Liu Cheng and Mittemeijer E J 1990 *Metall. Trans.* A **21** 13
[7] Mittemeijer E J, van Rooijen M, Wierszyllowski I and Rozendaal H C F 1983 *Z. Metallk.* **74** 473
[8] *Powder Diffraction File* 1967 (Philadelphia, PA: ASTM) card 6-0696
[9] Liu Cheng, van der Pers N M, Böttger A, de Keijser Th H and Mittemeijer E J 1990 *Metall. Trans.* at press
[10] MacGillavry C H, Rieck G D and Lonsdale K 1974 *International Tables for X-ray Crystallography* vol III (Birmingham: Kynoch)
[11] Lovesey S W 1984 *Theory of Neutron Scattering from Condensed Matter* vol 2 (Oxford: Clarendon)
[12] Shull C G and Yamada Y 1962 *J. Phys. Soc. Japan Suppl.* B **17** III 1
[13] Haije W G 1989 Netherlands Energy Research Foundation ECN, PO Box 1, 1755 ZG Petten, The Netherlands, private communication
[14] Delhez R, de Keijser Th H and Mittemeijer E J 1982 *Surf. Eng.* **3** 331
[15] Moss S C 1967 *Acta Metall.* **15** 1815
[16] Chen P C, Hall B O and Winchell P G 1980 *Metall. Trans.* A **11** 1323
[17] Krivoglaz M A 1969 *Theory of X-ray and Thermal-Neutron Scattering by Real Crystals* (New York: Plenum) p 228; 1959 *Phys. Met. Metallogr. (USSR)* **7** 11
[18] Van Gent A, Van Doorn F C and Mittemeijer E J 1985 *Metall. Trans.* A **16** 1371
[19] Guinier A 1963 *X-ray Diffraction in Crystals, Imperfect Crystals and Amorphous Bodies* (San Francisco, CA: Freeman) p 163
[20] Mori T, Cheng P C, Kato M and Mura T 1978 *Acta Metall.* **26** 1435
[21] Beshers D N 1973 *Diffusion* (Metals Park, OH: American Society for Metals) p 219